

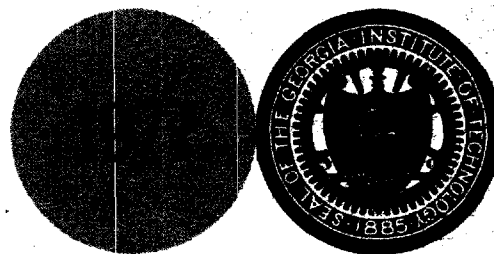
CONTRACT NAS8-31193

A LASER SCANNER FOR 35mm FILM

**W. R. Callen and J. E. Weaver
School of Electrical Engineering
Georgia Institute of Technology
Atlanta, Georgia 30332**

April 1977

FINAL REPORT FOR PERIOD 25 FEBRUARY 1975-24 APRIL 1977



Performed for:

**National Aeronautics and Space Administration
George C. Marshall Space Flight Center
Marshall Space Flight Center, Alabama 35812**

SCHOOL OF ELECTRICAL ENGINEERING
Georgia Institute of Technology
Atlanta, Georgia 30332

FINAL REPORT

PROJECT NO. E-21-657

A LASER SCANNER FOR 35 mm FILM

by

W. R. Callen and J. E. Weaver

RESEARCH CONTRACT NAS8-31193

25 February 1975 to 24 April 1977

Performed for

NATIONAL AERONAUTICS AND SPACE ADMINISTRATION
George C. Marshall Space Flight Center
Marshall Space Flight Center, Alabama 35812

ABSTRACT

This report describes the design, construction, and testing of a laser scanning system that was delivered to Marshall Space Flight Center. The scanner is designed to deliver a scanned beam over a 2.54 cm by 2.54 cm or a 5.08 cm by 5.08 cm format. In order to achieve a scan resolution and rate comparable to that of standard television, an acousto-optic deflector is used for one axis of the scan, and a light deflecting galvanometer is used for deflection along the other axis. The acousto-optic deflector has the capability of random access scan controlled by a digital computer.

TABLE OF CONTENTS

	<u>Page</u>
I. INTRODUCTION	1
II. OPTICAL SYSTEM DESIGN	3
A. Overall Approach	3
B. Laser Selection	3
C. Light Deflection System	3
1. Introduction	3
2. Acoustooptic Deflector	5
3. Description and Specifications of Acousto- Optic Beam Deflector	11
4. Galvanometer Deflector	13
D. Modulator	13
E. Scanner Controller	14
F. Focussing System and Alignment	14
III. SYSTEM EVALUATION	16
IV. A COHERENT LIGHT SCANNER FOR OPTICAL PROCESSING OF LARGE FORMAT TRANSPARENCIES	23
V. ACKNOWLEDGMENTS	31
REFERENCES	32

LIST OF FIGURES

<u>Figure</u>		<u>Page</u>
1	Schematic Diagram of Laser Scanner	4
2	Geometry of Bragg Scattering by Acoustic Wavefronts, Spaced a Distance λ_s Apart	7
3	Photon Picture for Bragg Scattering	8
4	Specifications for Acousto-Optic Beam Deflector	12
5	Formation of the Focussed Scan by a Lens	15
6	Laser Scanner in Operation	21
7	Scanned Pattern Obtained in the Sweep Mode of Operation of the Laser Scanner	22

I. INTRODUCTION

For experiments involving the processing of data stored as a two-dimensional scene, optical techniques are frequently convenient. The use of holographic techniques applied to nonlinear media has greatly expanded the potential for three dimensional high capacity optically based mass memories. The development of optical integrated circuits and miniature lasers and modulators has brought optical systems much closer to the realities of day-to-day existence.

Most laser systems used in the analysis of data or in the implementation of logical operations require some type of scanning system. In addition, many commercial systems, such as television displays, employ laser scanning systems [1-3].

Georgia Tech previously developed a laser scanning system useful in optical processing systems [4,5]. That scanner had two principal features:

1. The scanned beam was random access addressable, and was perpendicular to the image page.
2. The intensity of the scanned beam was controllable, such that constant light intensity could be maintained after passage through the image plane.

Because the above described scanner was optimized for optical processing applications, which require a non-focussed beam of high coherence, it employed a pair of light deflecting galvanometers coupled by a relay

mirror. The galvanometers were placed at the focus of a large diameter parabolic mirror. This system is described in Chapter IV of this report.

The scanning system developed under this contract was designed to provide a scanned focussed beam over a 2.54 cm by 2.54 cm format, or over a 5.08 cm by 5.08 cm format, with a resolution and rate comparable to that of standard television. As with most scanning systems, there is a trade-off between scanning rate and system resolution, within any given economic constraint. The result of this trade-off, as described in Chapter III of this report, is that a resolution equal to that of standard television was achieved, with a slightly lower scan rate than that of standard television. However, a higher scan rate can be achieved by reducing the scanned format. This type of scanner could be potentially useful as a flying spot scanner for video display of transparencies.

II. OPTICAL SYSTEM DESIGN

A. Overall Approach

A schematic diagram of the optical scanning system is shown in Figure 1. The laser output is controlled in irradiance by a Pockel's effect modulator. After the modulator, the beam passes through beam forming optics that tailor the shape of the beam for acceptance by the acousto-optic modulator, which provides one dimension of the scan. The other dimension of the scan is provided by a large light deflecting galvanometer. The resultant scanning beam is focussed by a lens onto the scan plane.

B. Laser Selection

Because of the increased sensitivity of film, nonlinear crystals and other recording media to light in the blue and green portion of the spectrum compared to that for light in the red portion of the spectrum, an argon laser is chosen as the design standard. The argon laser is the only commercially available laser capable of high power (greater than one watt), continuous-wave output in the blue or green region of the spectrum. In particular, our system is optimized for operation at 514.5 nm, one of the stronger output lines of the argon laser.

C. Light Deflection System

1. Introduction

The choice of light deflection systems for the laser scanner is principally influenced by the design goal of achieving a scan rate and resolution comparable to that of standard television. The scan of a

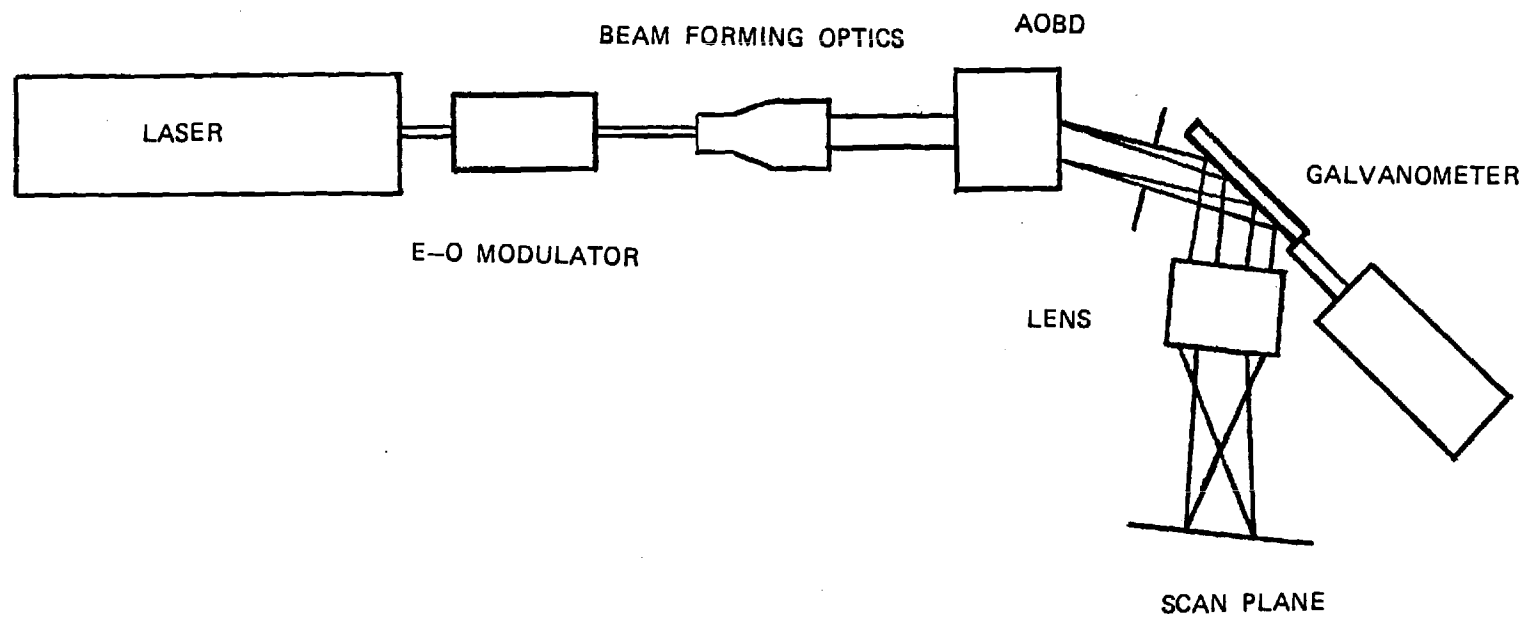


FIGURE 1. SCHEMATIC DIAGRAM OF LASER SCANNER

standard television operates at a rate of 525 lines per frame, with 30 frames per second, for 1.58×10^4 lines per second, which corresponds to a writing time of one line of 6.35×10^{-5} seconds. The required response time of the deflector is determined by this scan time of approximately 60 microseconds. The required detector bandwidth then is approximately the inverse of this, or 16 kilohertz. Standard television has approximately 600 resolvable spots.

Several types of scanning mechanisms can be considered for design of the scanner: (1) galvanometer (electromechanical) deflectors, (2) acoustooptic deflectors, and (3) electrooptic deflectors. For each type of deflector there are trade-offs with regard to resolution, access time, and cost. Among the three types, galvanometer deflectors offer high resolution and relatively slow access time for moderate cost, while electrooptic deflectors offer fast access time, but exhibit relatively poor resolution and are relatively expensive. Acoustooptic deflectors are an intermediate choice with regard to all three qualities at present. In general, galvanometer-based deflection systems are preferable because of ease of alignment, lack of beam distortion, and cost [6].

2. Acoustooptic Deflector

Since the performance of our system is based largely on that of the acoustooptic deflector, we review here some of the principal mechanisms underlying the operation of such a deflector. When a sound wave moves through a medium, a density variation and a corresponding variation in the index of refraction is produced [7]. This varying index of refraction acts as a series of "moving mirrors" inside the material. The moving mirrors are separated by a distance equal to the wavelength of

the sound in the medium. The plane of each mirror is perpendicular to the direction of the sound wave. For efficient diffraction of light from the moving mirrors to occur, two conditions must be met: (1) reflected light from any given portion of a mirror must add in phase with light reflected from a different portion of the mirror, and (2) reflections from two different mirrors (acoustic wave fronts) must add in phase. The first condition implies that the angle of incidence of the optical wave relative to the acoustic phase fronts must equal the angle of reflection. The second condition requires that the Bragg condition must be satisfied:

$$2\lambda_s \sin\theta = \lambda/n \quad , \quad (1)$$

where λ_s is the wavelength of the sound within the medium, θ is the angle of incidence within the crystal of the light beam with respect to the acoustic wavefronts, and λ/n is the free space wavelength of the light; the crystal has refractive index n . The geometry is shown in Figure 2.

The Bragg condition for light diffraction may be viewed as the annihilation of one photon representing the incident light wave and one photon representing the acoustic wave and the simultaneous creation of a new photon representing the diffracted wave. This is shown in Figure 3, where \vec{k}_i , \vec{k}_s , and \vec{k}_d represent the wave vectors of the incident light wave, the sound wave, and the diffracted light wave, respectively. Since $\omega_D = \omega_i + \omega_s \approx \omega_i$ and $\kappa_D \approx \kappa_i = K$, we therefore have that

$$\kappa_s = 2K \sin\theta, \quad \text{or} \quad (2)$$

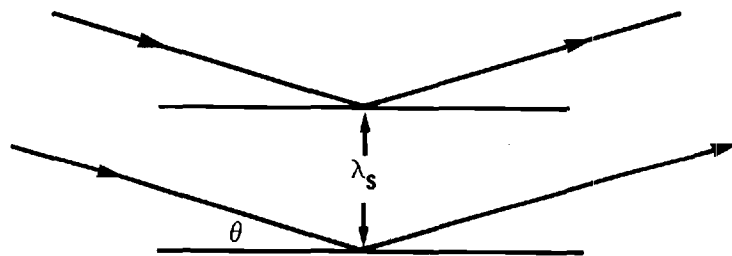


FIGURE 2. GEOMETRY OF BRAGG SCATTERING BY ACOUSTIC WAVEFRONTS, SPACED A DISTANCE λ_s APART.

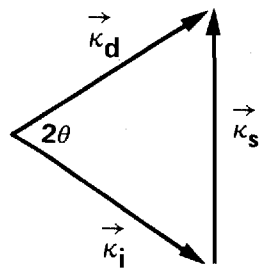


FIGURE 3. PHOTON PICTURE FOR BRAGG SCATTERING. THE INCIDENT LIGHT WAVE IS REPRESENTED BY $\vec{\kappa_i}$, THE DIFFRACTED WAVE BY $\vec{\kappa_d}$ AND THE ACOUSTIC WAVE BY $\vec{\kappa_s}$

$$2\lambda_s \sin\theta = \lambda/n \quad , \quad (3)$$

the Bragg condition stated earlier.

From the foregoing discussion, we see that for a given wavelength of light and frequency of the sound wave, there is a unique angle of incidence and diffraction. To achieve light deflection over an angular range, we select a sound frequency that corresponds to a deflection angle in the middle of the angular spread desired, and then adjust the incoming light beam to the corresponding angle of incidence. By then varying the sound frequency, a range of deflected angles is achieved. The change in the angle of diffraction is related to the change in frequency of the sound wave by [7]

$$\Delta\theta = \frac{\lambda\Delta\nu_s}{n\nu_s} \quad . \quad (4)$$

The number of resolvable spots N is equal to the ratio of $\Delta\theta$, the maximum deflection angle, to the full angle of the beam divergence, θ_d . The beam divergence θ_d is approximately λ/nD , where D is the beam diameter, so we have

$$N = \frac{\Delta\theta}{\theta_d} = \frac{\lambda\Delta\nu_s nD}{n\nu_s \lambda} = \Delta\nu_s \left(\frac{D}{\nu_s}\right) \quad , \quad (5)$$

or

$$N = \Delta\nu_s \tau \quad , \quad (6)$$

where τ is the time required for a sound wave to propagate across the diameter of the optical beam. This time-bandwidth product is a frequent specification of an acousto-optic deflector and gives a specification that is independent of the criterion used for a resolvable spot.

Usually for a light deflection system, we are interested not only in the angle of the reflected light, but in the amount of reflected light. From a consideration of nonlinear coupled wave equations describing the interaction of light and sound in the medium, it can be shown that the ratio of diffracted irradiance to incident irradiance is

$$\frac{I_{\text{diff}}}{I_{\text{in}}} = \sin^2 \frac{\pi l}{\sqrt{2} \lambda} \sqrt{M I_{\text{acoustic}}} , \quad (7)$$

where I_{acoustic} is the intensity of the acoustic wave, l is the interaction length, and M is a diffraction figure of merit. M is given by

$$M = \frac{n^6 p^2}{3 \rho v_s^3} , \quad (8)$$

where n is the refractive index, v_s the velocity of sound, ρ the mass density of the material, and p is the photoelastic constant. The value of M of telleriumdioxide (TeO_2), the material used in our deflector, relative to that of water is five.

Two principal sources of error in acoustooptic deflectors are (1) misadjustment of the Bragg angle, and (2) the deflector alignment is not correct over the entire angular range because of the varying frequencies that must be used. The first source of error is generally not significant. For example, a Bragg angle error on the order of 12% produces only

approximately a 5% reduction in intensity of the diffracted beam [8]. An interesting aspect of the second source of error is that a given percentage deviation in frequency above the center frequency causes a larger roll-off in intensity of the diffracted beam than does the same percentage deviation in frequency below the center frequency. The deflector can be made to exhibit equal intensity roll-off in both directions by aligning the beams at the Bragg angle at a frequency slightly higher than the center frequency.

3. Description and Specification of Acousto-Optic Beam Deflector

The specifications used in the purchase of the acousto-optic beam deflector are shown in Figure 4. The system can be operated in four distinct modes: manual, external input, sweep, and digital. The manual mode is operated by a ten turn potentiometer mounted on the driver. This potentiometer can vary the output frequency of the driver by approximately ± 250 KHz. The manual mode of operation yields a stationary deflected beam whose position can be varied by turning the potentiometer. The external input is operated by applying a voltage between zero and -8 volts, which in turn varies the RF output frequency. By applying a ramp or sawtooth external input from a function generator, scanning can be achieved. In the sweep mode, the driver automatically scans through a frequency range with the application of an external trigger pulse. The range of the frequency scan is determined by two potentiometers located on the front panel of the driver.

The digital mode requires a 12 bit digital input, with the first bit the most significant bit and the twelfth bit the least significant bit. A digital input of all zeroes corresponds to a driver output

SPECIFICATIONS - ACOUSTO-OPTIC BEAM DEFLECTOR

Deflector

Aperture	50 mm maximum
Laser input	514.5 nm, less than 1 watt
Time-bandwidth product	Greater than 750
Deflection efficiency	Greater than 30%; less than 3 db variation over full swing of deflected beam

Driver

Positioning modes	Manual - from panel front Analog - 0 to 5 volt full swing input. Deflection angle must be linear with input voltage; the maximum deviation from a linear voltage-angle relationship must be less than .025% of the full angular swing. Digital input - 9 bit TTL parallel addressing for 512 uniformly separated angular positions. (Less than 1 spot to spot center spacing variation.) Clock input - for stair step scan.
Maximum input power	120 vac, 15 amps, 1 ϕ

Mechanical

Deflector and driver must be separate units. Driver must be rack mountable. Deflector must have provisions (tapped holes) for mounting.

FIGURE 4. SPECIFICATIONS FOR ACOUSTO-OPTIC BEAM DEFLECTOR.

frequency of 62.72 MHz, while an input of all ones corresponds to a driver output frequency of 131.16 MHz. The entire digital input-output table is included in Chapter III, System Evaluation.

The detailed operating manuals that accompany the acousto-optic deflector and driver are included under separate cover [9,10].

4. Galvanometer Deflector

In order to achieve a scan rate comparable to standard television, the horizontal deflector must be able to scan at a rate such that 30 frames per second are displayed. One of the fastest and cheapest electromechanical systems is that of a light deflecting galvanometer. The galvanometer acts as a driven angular oscillator with a driving term proportional to the current. The result for a critically damped galvanometer is that, within the range of application, a deflection angle proportional to current is obtained. To obtain a full scan in $1/30$ (.03) of a second, the galvanometer must be able to swing twice its full deflection angle in $1/30$ second. The galvanometer chosen for our system is the General Scanning Model 320 PD, which is capable of a 20° mechanical rotation, peak-to-peak. This model has a resonant frequency of 165 Hz, and can be driven sinusoidally at up to 85% of its frequency, or 140 Hz, which corresponds to a period of .007 seconds, well within the .03 second scan requirement [11-13].

D. Modulator

In order to achieve a beam pattern that has intensity variation, a modulator must be employed. In order to be able to write 500 resolvable spots in each dimension at standard television rates, the modulator must be able to respond to a signal whose period is equal to the active write

time of standard television divided by 250 (500 resolvable spots corresponds to 250 full cycles), or $T = 56 \times 10^{-6} \text{ sec} / 250 = 2.24 \times 10^{-7} \text{ sec}$. This corresponds to a bandwidth requirement of 4.46 MHz. The only modulator available for use in our system is the Coherent Associates Model 3003 Modulation System, which has a bandwidth of 3 MHz, and therefore provides the limiting factor in our system [14].

E. Scanner Controller

The driver for the acoustooptic beam deflector may be controlled by a microcomputer system. The KIM-1 microcomputer system, from MOS Technology, Inc. is included with the laser scanner.

F. Focussing System Alignment

In order to fill the aperture of the acousto-optic beam deflector, the laser beam is expanded and collimated by a pair of lenses whose focal lengths are in the ratio $\frac{200 \text{ mm}}{3 \text{ mm}}$. The light deflecting galvanometer is placed almost as close as possible to the output aperture of the acousto-optic beam deflector. This eliminates the need for any relaying optics, and the resultant beam behaves as if it were a collimated beam emanating from a single two-axis deflector. A focussed raster scan is obtained by placing a lens at the output of the deflector pair. The format size d is related to the full angle beam divergence θ as shown in Figure 5, by

$$d = 2f \tan \theta/2 \quad , \quad (9)$$

which for small angles reduces to

$$d = f\theta \quad . \quad (10)$$

For a square scan format, each deflector should swing through the same angle, and a cylindrically symmetric lens can be used.

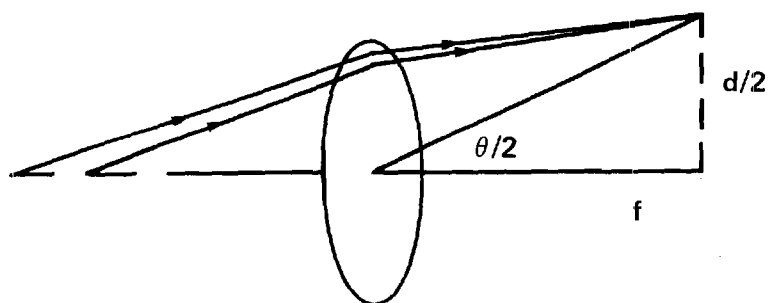


FIGURE 5. FORMATION OF THE FOCUSED SCAN BY A LENS. THE DEFLECTOR ANGLE HAS A FULL ANGLE OF DEFLECTION OF θ AND FORMS A PATTERN OF SIDE d IN LENGTH.

III. SYSTEM EVALUATION

The system was aligned as discussed in Chapter III, Section 8, and a lens was employed to obtain a focussed format. A picture of the experimental arrangement is shown in Figure 6.

The focussing lens had a focal length of 500 mm and each deflector operated through a full angular swing of approximately .06 radians. From Equation 10, the resultant format size is approximately $d = .06(500) = 30$ mm.

The system was operated in the manual, sweep, and external input modes of operation. Square raster patterns were obtained in both the sweep and external input modes of operation. The pattern obtained in the sweep mode when the galvanometer operated at a rate of 24 Hz and the acousto-optic beam deflector at a rate of 11.43 KHz is shown in Figure 7. In the sweep mode, the acousto-optic beam deflector seemed to exhibit nonlinearities around 12 KHz. In the external input mode, however, a square raster pattern of approximately even irradiance was obtained using a ramp function of frequency 15.775 KHz, approximately the rate of standard television. In the external input mode, the upper frequency limit of operation before nonlinearities in the pattern appeared was about 16 KHz. Detailed data sheets from the manufacturer are shown on the next four pages.

		<h1 style="margin: 0;">TEST DATA SHEET</h1>		ACOUSTO-OPTIC DRIVER	
TEST PROCEDURE NO.	SOURCE CONTROL DRAWING	MODEL NO. <u>D 101-2</u>	SERIAL NO. <u>1420</u>		
CODE IDENT NO. 07720	CUSTOMER P.O. NO. <u>0000</u>	TESTED BY	DATE <u>8 MAR 77</u>		

MANUAL TUNE MODE

Manual Tune Potentiometer	Driver Output Frequency	Driver Output Power (Max.)
000	<u>62.85</u> MHz	<u>2.8 w</u>
100	<u>70.32</u> MHz	<u>3.0 w</u>
200	<u>77.26</u> MHz	<u>3.1 w</u>
300	<u>83.93</u> MHz	<u>2.1 w</u>
400	<u>90.69</u> MHz	<u>3.0 w</u>
500	<u>97.38</u> MHz	<u>2.9 w</u>
600	<u>103.96</u> MHz	<u>3.0 w</u>
700	<u>110.62</u> MHz	<u>3.2 w</u>
800	<u>117.10</u> MHz	<u>3.4 w</u>
900	<u>124.08</u> MHz	<u>3.4 w</u>
000	<u>131.33</u> MHz	<u>3.2 w</u>

EXTERNAL INPUT MODE

Ext Input Voltage	Driver Output Frequency	Driver Output Power (Max.)
0.00 volts	<u>62.67</u> MHz	<u>3.0 w</u>
-1.00 volts	<u>75.733</u> MHz	<u>3.4 w</u>
-2.00 volts	<u>88.243</u> MHz	<u>3.2 w</u>
-3.00 volts	<u>100.474</u> MHz	<u>3.3 w</u>
-4.00 volts	<u>112.766</u> MHz	<u>3.5 w</u>
-5.00 volts	<u>125.405</u> MHz	<u>3.4 w</u>
-6.00 volts	_____ MHz	_____
-7.00 volts	_____ MHz	_____
-8.00 volts	_____ MHz	_____
-9.00 volts	_____ MHz	_____
-10.00 volts	_____ MHz	_____

AUTO SCAN MODE

Lower Freq. Limit 63.67 MHz - 87.96 MHz
 Upper Freq. Limit 84.83 MHz - 131.15 MHz
 Sweep Output 0 Volts to -5.4 volts Max.

Operator Notes:

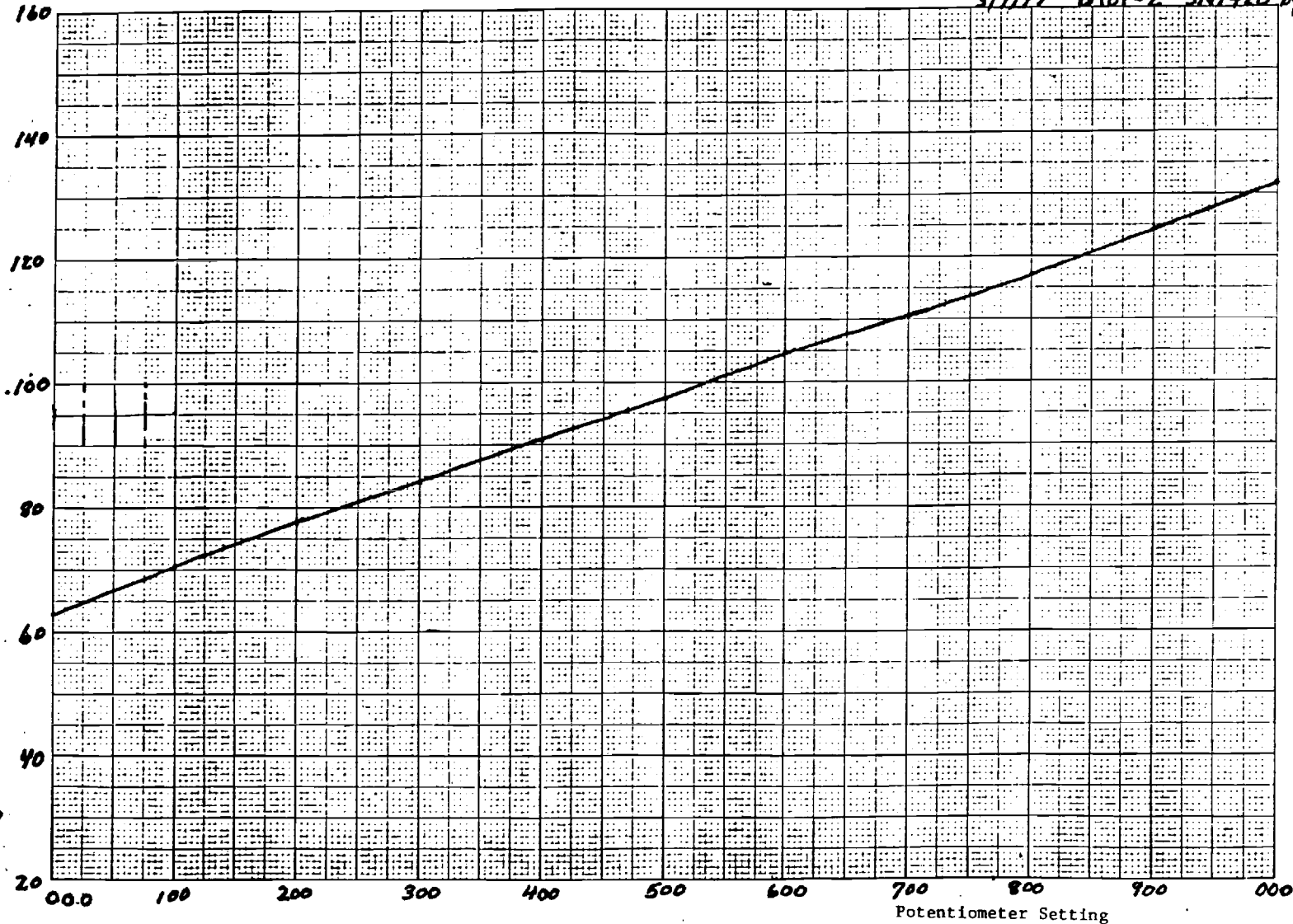
All test data taken after a one (1) hour warm up period.

CSI APPROVAL	DATE	ISOMET QC APPROVAL	DATE	PAGE OF
			<u>3-25-77</u>	

ISOMET		TEST DATA SHEET		ACOUSTO-OPTIC DRIVER																																																																																																																																																																																																																			
TEST PROCEDURE NO.	SOURCE CONTROL DRAWING	MODEL NO.	SERIAL NO.																																																																																																																																																																																																																				
		D101- 2	1120																																																																																																																																																																																																																				
CODE IDENT NO. 07720	CUSTOMER P.O. NO.	TESTED BY	DATE																																																																																																																																																																																																																				
		00	3/7/77																																																																																																																																																																																																																				
TEST DATA - DIGITAL OPTION																																																																																																																																																																																																																							
(1MSB,) (12LSB)	<table style="width: 100%; border-collapse: collapse;"> <thead> <tr> <th colspan="12" style="text-align: center;">DIGITAL INPUT</th> <th style="text-align: center;">OUTPUT FREQUENCY MHz</th> <th style="text-align: center;">DRIVER OUTPUT PWR (WATTS)</th> </tr> <tr> <th>1</th><th>2</th><th>3</th><th>4</th><th>5</th><th>6</th><th>7</th><th>8</th><th>9</th><th>10</th><th>11</th><th>12</th> <th></th> <th></th> </tr> </thead> <tbody> <tr><td>0</td><td>0</td><td>0</td><td>0</td><td>0</td><td>0</td><td>0</td><td>0</td><td>0</td><td>0</td><td>0</td><td>0</td><td>62.72</td><td>3.0W</td></tr> <tr><td>0</td><td>0</td><td>0</td><td>0</td><td>0</td><td>0</td><td>0</td><td>0</td><td>0</td><td>0</td><td>0</td><td>1</td><td>62.73</td><td>3.0W</td></tr> <tr><td>0</td><td>0</td><td>0</td><td>0</td><td>0</td><td>0</td><td>0</td><td>0</td><td>0</td><td>0</td><td>1</td><td>1</td><td>62.76</td><td>3.0W</td></tr> <tr><td>0</td><td>0</td><td>0</td><td>0</td><td>0</td><td>0</td><td>0</td><td>0</td><td>0</td><td>1</td><td>1</td><td>1</td><td>62.83</td><td>3.0W</td></tr> <tr><td>0</td><td>0</td><td>0</td><td>0</td><td>0</td><td>0</td><td>0</td><td>0</td><td>1</td><td>1</td><td>1</td><td>1</td><td>62.96</td><td>3.0W</td></tr> <tr><td>0</td><td>0</td><td>0</td><td>0</td><td>0</td><td>0</td><td>1</td><td>1</td><td>1</td><td>1</td><td>1</td><td>1</td><td>63.25</td><td>3.0W</td></tr> <tr><td>0</td><td>0</td><td>0</td><td>0</td><td>0</td><td>1</td><td>1</td><td>1</td><td>1</td><td>1</td><td>1</td><td>1</td><td>63.81</td><td>3.0W</td></tr> <tr><td>0</td><td>0</td><td>0</td><td>0</td><td>1</td><td>1</td><td>1</td><td>1</td><td>1</td><td>1</td><td>1</td><td>1</td><td>64.94</td><td>3.1W</td></tr> <tr><td>0</td><td>0</td><td>0</td><td>1</td><td>1</td><td>1</td><td>1</td><td>1</td><td>1</td><td>1</td><td>1</td><td>1</td><td>67.19</td><td>3.2W</td></tr> <tr><td>0</td><td>0</td><td>1</td><td>1</td><td>1</td><td>1</td><td>1</td><td>1</td><td>1</td><td>1</td><td>1</td><td>1</td><td>71.62</td><td>3.2W</td></tr> <tr><td>0</td><td>1</td><td>1</td><td>1</td><td>1</td><td>1</td><td>1</td><td>1</td><td>1</td><td>1</td><td>1</td><td>1</td><td>80.26</td><td>3.2W</td></tr> <tr><td>0</td><td>1</td><td>1</td><td>1</td><td>1</td><td>1</td><td>1</td><td>1</td><td>1</td><td>1</td><td>1</td><td>1</td><td>96.99</td><td>3.0W</td></tr> <tr><td>1</td><td>1</td><td>1</td><td>1</td><td>1</td><td>1</td><td>1</td><td>1</td><td>1</td><td>1</td><td>1</td><td>1</td><td>131.16</td><td>3.3W</td></tr> </tbody> </table>					DIGITAL INPUT												OUTPUT FREQUENCY MHz	DRIVER OUTPUT PWR (WATTS)	1	2	3	4	5	6	7	8	9	10	11	12			0	0	0	0	0	0	0	0	0	0	0	0	62.72	3.0W	0	0	0	0	0	0	0	0	0	0	0	1	62.73	3.0W	0	0	0	0	0	0	0	0	0	0	1	1	62.76	3.0W	0	0	0	0	0	0	0	0	0	1	1	1	62.83	3.0W	0	0	0	0	0	0	0	0	1	1	1	1	62.96	3.0W	0	0	0	0	0	0	1	1	1	1	1	1	63.25	3.0W	0	0	0	0	0	1	1	1	1	1	1	1	63.81	3.0W	0	0	0	0	1	1	1	1	1	1	1	1	64.94	3.1W	0	0	0	1	1	1	1	1	1	1	1	1	67.19	3.2W	0	0	1	1	1	1	1	1	1	1	1	1	71.62	3.2W	0	1	1	1	1	1	1	1	1	1	1	1	80.26	3.2W	0	1	1	1	1	1	1	1	1	1	1	1	96.99	3.0W	1	1	1	1	1	1	1	1	1	1	1	1	131.16	3.3W
DIGITAL INPUT												OUTPUT FREQUENCY MHz	DRIVER OUTPUT PWR (WATTS)																																																																																																																																																																																																										
1	2	3	4	5	6	7	8	9	10	11	12																																																																																																																																																																																																												
0	0	0	0	0	0	0	0	0	0	0	0	62.72	3.0W																																																																																																																																																																																																										
0	0	0	0	0	0	0	0	0	0	0	1	62.73	3.0W																																																																																																																																																																																																										
0	0	0	0	0	0	0	0	0	0	1	1	62.76	3.0W																																																																																																																																																																																																										
0	0	0	0	0	0	0	0	0	1	1	1	62.83	3.0W																																																																																																																																																																																																										
0	0	0	0	0	0	0	0	1	1	1	1	62.96	3.0W																																																																																																																																																																																																										
0	0	0	0	0	0	1	1	1	1	1	1	63.25	3.0W																																																																																																																																																																																																										
0	0	0	0	0	1	1	1	1	1	1	1	63.81	3.0W																																																																																																																																																																																																										
0	0	0	0	1	1	1	1	1	1	1	1	64.94	3.1W																																																																																																																																																																																																										
0	0	0	1	1	1	1	1	1	1	1	1	67.19	3.2W																																																																																																																																																																																																										
0	0	1	1	1	1	1	1	1	1	1	1	71.62	3.2W																																																																																																																																																																																																										
0	1	1	1	1	1	1	1	1	1	1	1	80.26	3.2W																																																																																																																																																																																																										
0	1	1	1	1	1	1	1	1	1	1	1	96.99	3.0W																																																																																																																																																																																																										
1	1	1	1	1	1	1	1	1	1	1	1	131.16	3.3W																																																																																																																																																																																																										
ANALOG V ALL 1S - 5.41 ANALOG V ALL OS - 1.0 mV																																																																																																																																																																																																																							
CSI APPROVAL		DATE	ISOMET QC APPROVAL		DATE																																																																																																																																																																																																																		
			QCE		3/7/77																																																																																																																																																																																																																		
3-7-77					PAGE OF																																																																																																																																																																																																																		

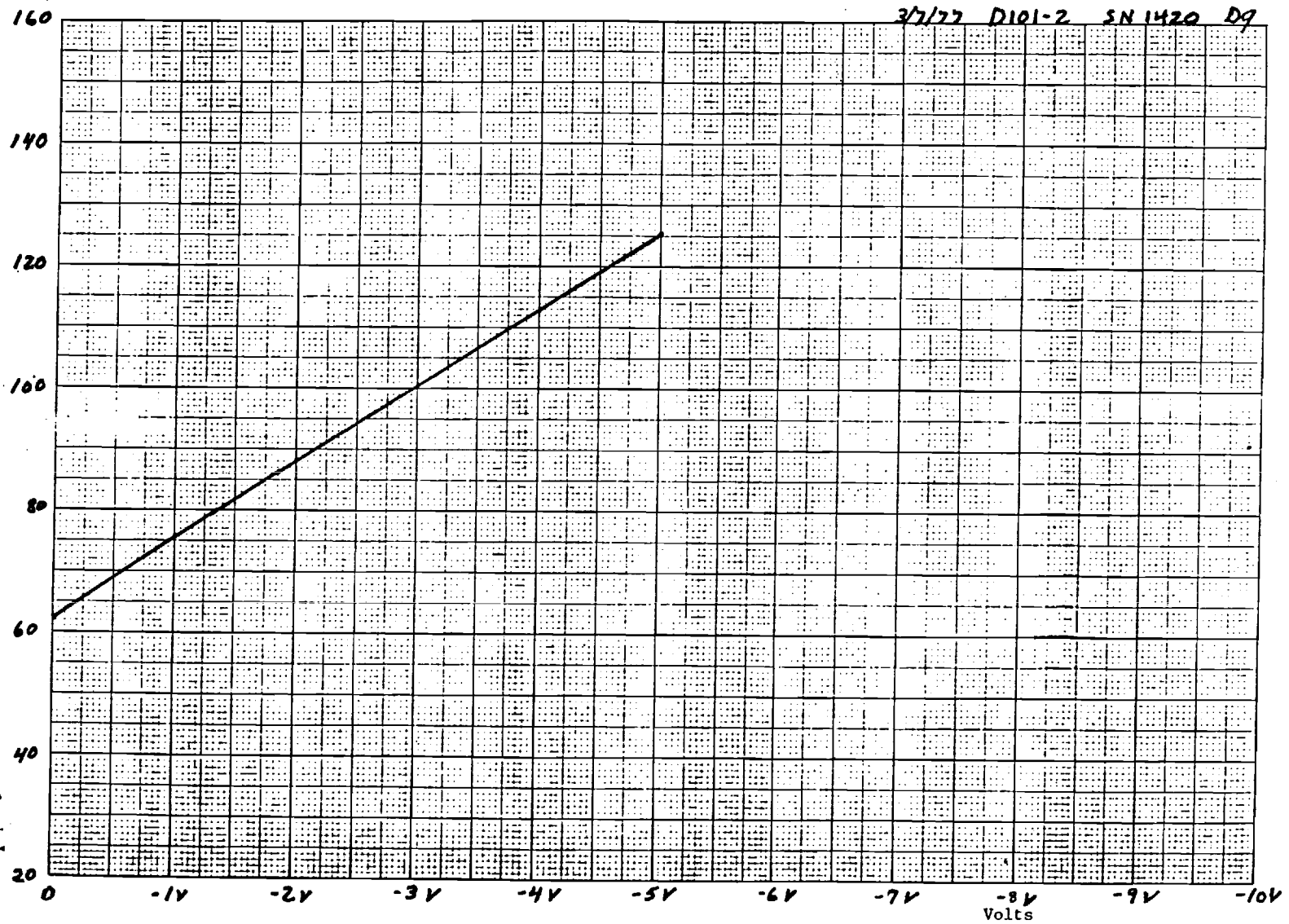
OUTPUT
FREQ. MHz

3/7/77 D101-2 SN1420 Dg



OUTPUT
FREQ MHz

3/7/77 D101-2 SN 1420 D9



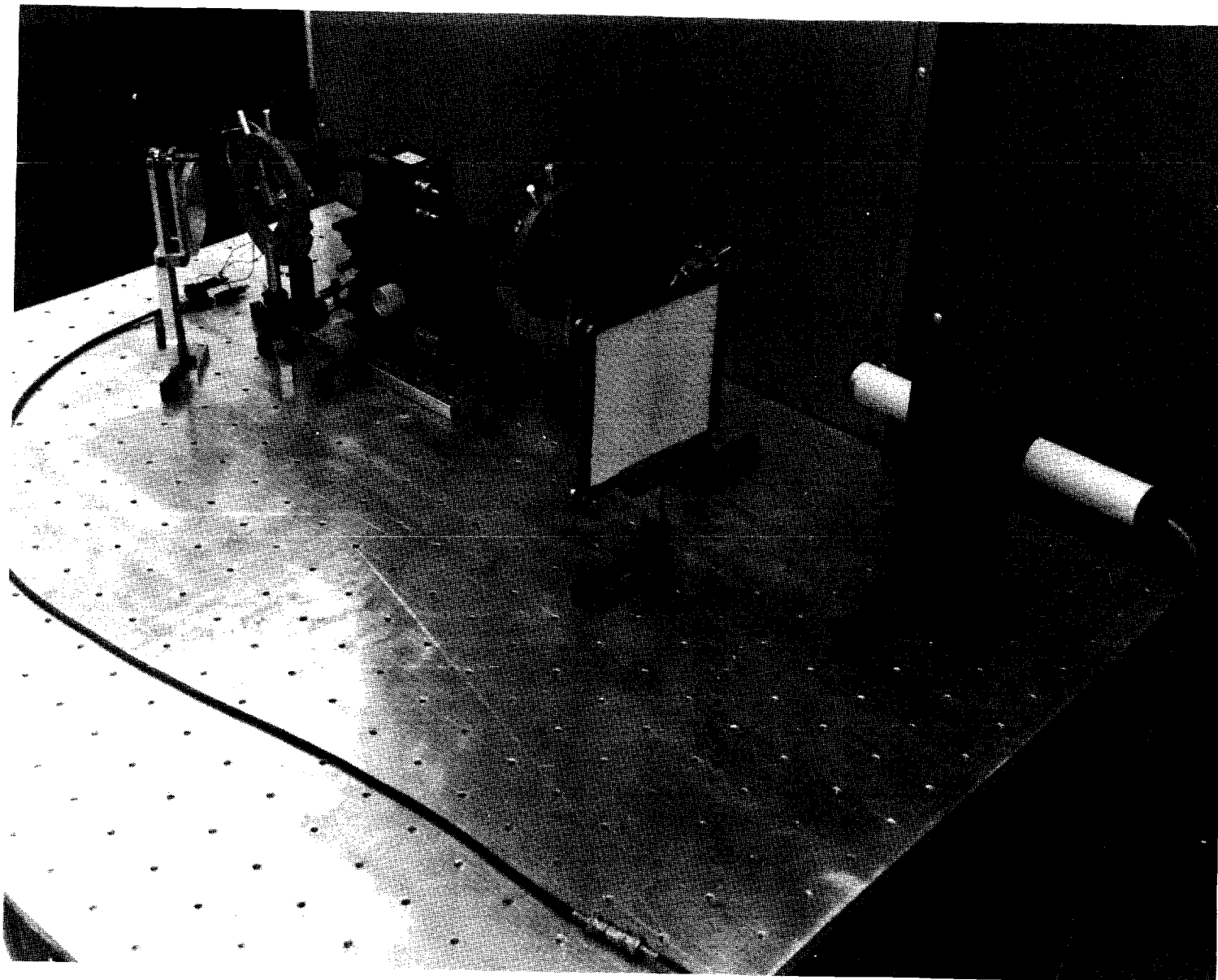


FIGURE 6. LASER SCANNER IN OPERATION.

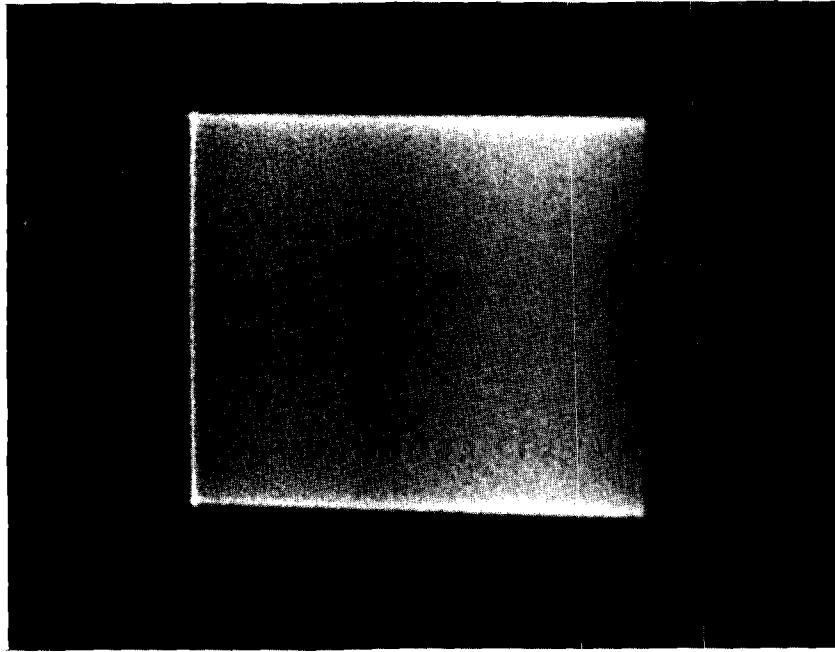


FIGURE 7. SCANNED PATTERN OBTAINED IN THE SWEEP MODE OF OPERATION OF THE LASER SCANNER.

IV. A COHERENT LIGHT SCANNER FOR OPTICAL PROCESSING OF LARGE FORMAT TRANSPARENCIES

A coherent light scanner for optical processing of large format transparencies was developed under a previous NASA contract with the Georgia Institute of Technology, Contract No. NAS8-28591, but was officially reported in the literature [5] during the contracting period that is the subject of this report. Since some of the considerations discussed there have bearing on the general topic of laser scanner development, Reference [5] is duplicated herein.

A COHERENT LIGHT SCANNER FOR OPTICAL
PROCESSING OF LARGE FORMAT TRANSPARENCIES

by

W. R. Callen and J. E. Weaver
School of Electrical Engineering
Georgia Institute of Technology
Atlanta, Georgia

and

R. G. Shackelford and J. R. Walsh
Engineering Experiment Station
Georgia Institute of Technology
Atlanta, Georgia

Introduction

Optical techniques are desirable for experiments involving the processing of large amounts of data stored as a two dimensional scene. Processing by computer usually requires digitizing an image and performing a two-dimensional Fourier transform numerically, which may be both costly and time-consuming. A schematic diagram of a standard optical processing system used for pattern recognition is shown in Figure 1.¹ The image to be processed is placed in the image plane of the processor and is illuminated by a coherent beam of light, as from a laser. The image can be in the form of film or can be produced by an image forming light modulator controlled by computer.^{2,3} The spatial Fourier transform of the input image appears in the focal plane of the first transform lens.⁴

If no additional elements are incorporated in the optical processor, the inverted image appears in the back focal plane of the second transform lens. By placing a matched filter of a second image in the transform plane, the spatial correlation of the two images appears in the output plane. The matched filter, which is a holographic record of the Fourier transform of the second image, can be produced by either optical or computer methods. The degree of correlation of the transform of the input image with that of the matched filter in the transform plane is indicated by the light irradiance distribution in the output plane. If the input image is not centered on the optical axis, the correlation plane irradiance distribution shifts by a distance proportional to the misregistration distance.

Illumination of the input image can be accomplished by two principal approaches:

1. illumination of the entire transparency, or
2. illumination of an area smaller than the transparency format, and then scanning over the entire format, repeating the optical data processing operation at each location.

The first approach--illumination of the entire transparency--necessitates the use of large aperture collimating optics and a powerful laser. The position of objects in the input plane is determined by a detector array or correlation plane scanner. Although the second approach requires a parallel scanning beam, it does not require the use of large aperture optics or a powerful laser. By collecting the light over a region of the correlation plane, the position of the portion of the image that correlates with the matched filter can be determined from the position of the scanning beam at the time that a relative maximum is detected in the correlation plane. Thus, correlation plane scanning may be eliminated.

A conceptual design of a traffic pattern analyzer using optical correlation is illustrated in Figure 2. Although this system is not meant to describe an actual on-line traffic analyzer, it exhibits features common to many correlator-based systems. The film transport contains the aerial photographs to be processed. The marginal information associated with the aerial photographs--

altitude, time, and possibly position and azimuth--can be stored as a data block that is automatically read at the film transport and entered into the computer. The computer positions the film for a desired frame and controls the laser scanner to examine a prescribed path, e.g., a highway. The holographic filter is the matched filter against which the aerial photographs is searched for the presence or absence of a vehicle or other object of interest.

The television display of the film being processed is strictly for operator convenience. At any single laser scanner position, the correlation plane may be scanned to examine the intensity contours of spots in the correlation plane for further identification.

Ideally, the operator of such a system would be able to instruct the processor to count the number of vehicles travelling in a certain direction in a given area at a specific time. Individual positions of distinct vehicles could be recorded. By examining the change in position of a number of vehicles on two consecutive frames taken a few seconds apart, an estimate of traffic flow could be determined. Such a system would allow traffic engineers to recover and process vast amounts of traffic data in a short time.

Many approaches have been employed to develop laser scanners for such diverse applications as writing television images, recording images on film, and storing data in optical memories. Most of these scanners are optimized by reducing the area of the beam and by increasing the bandwidth of the positioning mechanism. Unlike the types of scanners mentioned above, accurate random access positioning and beam parallelism are necessarily emphasized for a scanner to be used in an optical data processing application. Although the choice of deflectors for a system application may not be simple, galvanometer type deflectors offer higher resolution and beam quality, with a corresponding sacrifice in access time, compared to electro-optic and acousto-optic deflectors.⁵ Rotating polygonal mirror systems are useful for many video rate scanning operations, but are not random access by nature and, in general, are significantly more expensive. The laser scanner discussed below has the following novel features:

1. the scanning beam is random access addressable and is perpendicular to the input image plane, and
2. the irradiance of the scanned beam is controlled such that a constant average irradiance is maintained after passage through the image plane.

Optical System

A schematic diagram of the laser scanner is shown in Figure 3. The laser output irradiance is controlled by a Pockel's cell modulator. The beam passes through a spatial filter, is expanded and recollimated, and then is reduced to the desired diameter by an adjustable aperture assembly. The laser beam is then focussed onto a light deflection system that acts as a flat mirror with two angular degrees of freedom. The deflected and diverging beam is collimated by an off axis paraboloidal section. The collimated beam is then directed parallel to the optical axis by the paraboloidal section.

To deflect the beam effectively in two angular degrees of freedom, two flat mirrors mounted on the rotating shafts of moving iron galvanometers and a spherical relay mirror are used. The beam from the laser is focussed to a spot on the axis of rotation of the horizontal deflecting galvanometer mirror. The diverging beam is collected by a spherical mirror, positioned such that the center of curvature is slightly to one side of the focussed spot. The light reflected by the spherical mirror then images the focussed spot at an equal distance on the opposite side of the center of curvature, with unity magnification. By placing the axis of the second moving iron galvanometer mirror at this point, two dimensional deflection from a point is obtained. By employing controllable galvanometer deflections, random access to any position in the scanned format is possible.

Optical Design

To analyze the design of the scanner, we consider the collimated parallel scanning beam that passes through the transparency and works backward toward the laser. To avoid occultation of the scanned format by the deflector mirrors, an off-axis parabolic section is used. Our system is designed for scanning over a 10.0 cm by 10.0 cm format. As shown in Figure 4, half of a parabolic mirror of 33.0 cm diameter is quite adequate. A focal length of 115 cm was chosen because of the significant increase of cost for lower f-number. Interferograms of both sections after cutting indicated a deviation of

less than $\lambda/10$ over the scanned portion of the mirror.

The required format dimension of 10.0 cm and the parabola focal length of 115 cm require that the deflectors scan through a half-angle of approximately two and one-half degrees, which is compatible with standard deflectors. (A maximum half-angle scan of three degrees requires a minimum focal length of the parabola of 96 cm.)

In the previous discussion of the overall system, we indicated that the two axis deflection is obtained by closely positioning two orthogonal galvanometers on opposite sides of the center of curvature of a relay spheroidal mirror. The circular deflector mirrors can be positioned with a minimum center-to-center separation of 4 mm. The f-number of the spherical relay mirror must be low enough to accommodate the deflection angle of the galvanometers, and the focal length must be long compared to the separation between galvanometers. A focal length of 30.5 cm results in the two focused spots being 3.3 milliradians off axis, which produces negligible aberrations. A half angle scan of three degrees requires that the f-number be less than $(\frac{1}{2} \sin 3^\circ)$, or approximately F/5. An F/4 spheroid was fabricated from a standard 76 mm (3 inch) diameter optical blank. A slower mirror could have been used, but an F/4 mirror was chosen to eliminate possible problems with edge effects due to mounting and surface finish. The central 60 mm of this mirror is spherical in shape within a tolerance of $\lambda/5$.

The galvanometer light deflectors are mounted in a fixture that allows fine orthogonal positioning. A single thin lens of focal length 110 cm is used to focus the beam on the first galvanometer mirror axis. Preceding the thin lens is a spatial filter and collimator assembly using standard commercial optics mounted in a modified holder for long-term positioning stability. Any one of a series of circular apertures 1.2 mm to 10 mm in diameter mounted on interchangeable metal slides can be placed immediately behind the collimating lens to vary the beam diameter. The beam diameter must be greater than the largest dimension of the object being searched for in the image plane. Figure 5 illustrates how this would be determined for an aerial photograph of an automobile. From the figure,

$$\text{Beam diameter} \approx \text{object size} \times \frac{\text{focal length}}{\text{aircraft height}} \quad (1)$$

As an example, an object diameter of 10.7 meters (35 feet) photographed by an aircraft at a height of 610 meters (2000 feet) using a .305 m (12 inch) focal length lens requires a beam diameter of approximately 5.4 mm.

Between the laser and spatial filter is an on-off shutter and Pockel's effect modulator to control the beam irradiance. A feedback system has been designed to maintain constant average irradiance in the beam after passage through the film transparency. This feedback system can correct for local variations in the average film optical density. The laser used in the system is an argon ion laser capable of TEM₀₀ output of approximately 800 mW at 514.5 nm or 300 mW at 488.0 nm.

System Performance

The response time of the scanner is essentially determined by the response of the galvanometer driven mirrors, as they are much slower than any other component. To measure the response time, a step voltage is applied to the galvanometer. The galvanometer contains a position detector circuit that delivers a current in direct proportion to the mirror deflection. By displaying the response to a square wave and the square wave itself on a storage oscilloscope, the response time of the galvanometer is estimated to be approximately two milliseconds.

A more significant test of the scanner's performance is that of beam parallelism and spot size variation during the scanning process. By directly measuring the Fourier transform as the beam scans, the effect of both factors can be observed. The test procedure is shown in Figure 6. The scanning beam was focussed to a spot by a F/3.5, 45 cm focal length Cooke triplet. The spot was imaged by a microscope on a ground glass camera back. The spot, when examined with the beam stationary, was an Airy disc pattern. With the beam scanning at a horizontal rate of 700 Hz and a vertical rate of 28 Hz, no motion of the transform was detected visually. Several one second time exposure photographs were taken, as shown in Figure 7, corresponding to an enlargement of 63.5 diameters. From the photo and from visual inspection, we estimate that the shift in the pattern is less than 1/10 of the radius.

of the first dark ring. For the 2.7 mm aperture, the radius of the first dark ring is 6.0 mm, which results in a shift of

$$\Delta X < .1 \times \frac{6.0 \text{ mm}}{63.5} < 10\mu \quad (2)$$

A positional shift in the transform corresponds to an angular deviation of the scanner of

$$\Delta\theta = \frac{\Delta X}{f} < \frac{10^{-5} \text{ m}}{45.7 \times 10^{-2} \text{ m}} \quad (3)$$

or

$$\Delta\theta < 2 \times 10^{-5} \text{ radians.} \quad (4)$$

A photograph of the scanner in operation is shown in Figure 8.

Conclusion

The successful operation of a laser scanner that is constructed from readily available components of modest cost indicates further progress in the development of hybrid optical-digital processing schemes. The scanner has been demonstrated to exhibit the degree of spatial invariance necessary for certain optical processing applications. Data in the form of large format transparencies can be processed without the expense, space, maintenance, and precautions attendant to the operation of a high power laser with large aperture collimating optics. The scanned format and scanning beam diameter may be increased by simple design modifications. By employing acousto-optic deflectors with different relay optics, higher scan rates can be achieved, at the sacrifice of resolution.

Acknowledgements. This work was developed under NASA Contract NAS8-28591. We would like to express appreciation to Mr. Joe Kerr, Mr. Frayne Smith, and Mr. Ellington Pitts of NASA/MSFC and to Mr. John York and Mr. Bill Evans of Sperry Rand Corporation, Space Support Division for their assistance and support.

References

1. A. Vander Lugt, "Coherent Optical Processing," Proc. IEEE, vol. 62, pp. 1300-1317, October 1974.
2. David Casasent, "The Optical-Digital Computer," Laser Focus, vol. 7, pp. 30-33, September 1971.
3. R. G. Shackelford and J. R. Walsh, "Design and Fabrication of an Experimental Image Forming Light Modulator," NASA Technical Brief No. B73-10182, June 1973.
4. J. W. Goodman, Introduction to Fourier Optics, New York: McGraw-Hill, 1968.
5. J. David Zook, "Light Beam Deflector Performance: A Comparative Analysis," Appl. Optics, vol. 13, pp. 875-887, April 1974.

W. Russell Callen is an assistant professor in the School of Electrical Engineering at Georgia Tech. His research specialties are electro-optical systems and laser physics, and he is currently co-authoring a laser textbook.

John E. Weaver is a Ph.D. candidate in the School of Electrical Engineering at Georgia Tech. He previously was a physicist at Sperry Rand Corporation, Space Support Division, Huntsville, Alabama.

Robert G. Shackelford is Head of the Electro-Optics Group of the Engineering Experiment Station at Georgia Tech. His background includes research and development on systems and components for coherent optical data processing and laser communications.

Joseph R. Walsh is a Senior Research Engineer at the Engineering Experiment Station at Georgia Tech. His background includes research and development related to communication systems, digital processing and optical data processing.

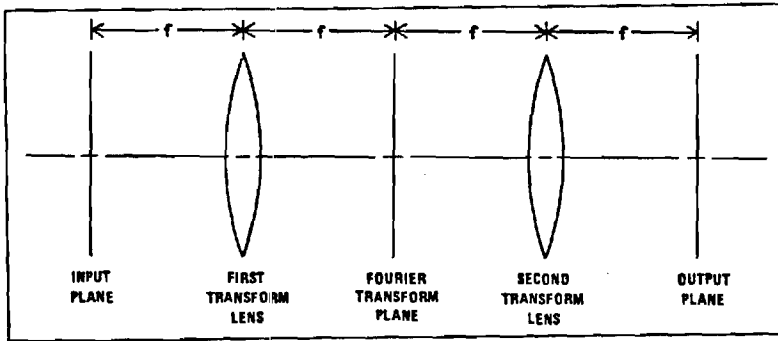


Fig. 1. Basic optical processor.

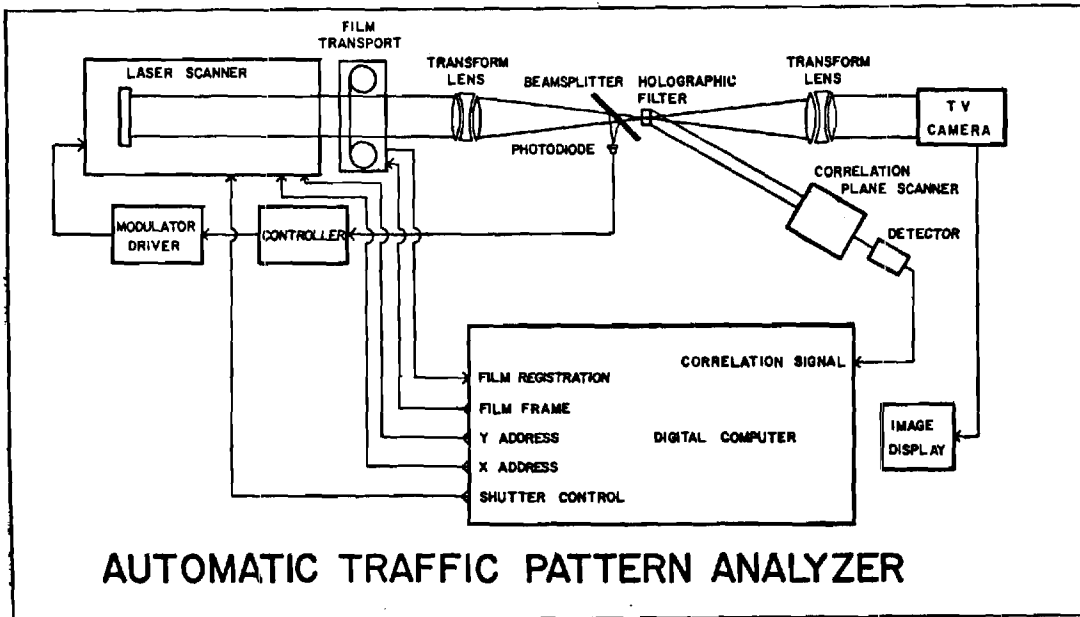


Fig. 2. Example of a hybrid optical-digital processor for analysis of traffic patterns.

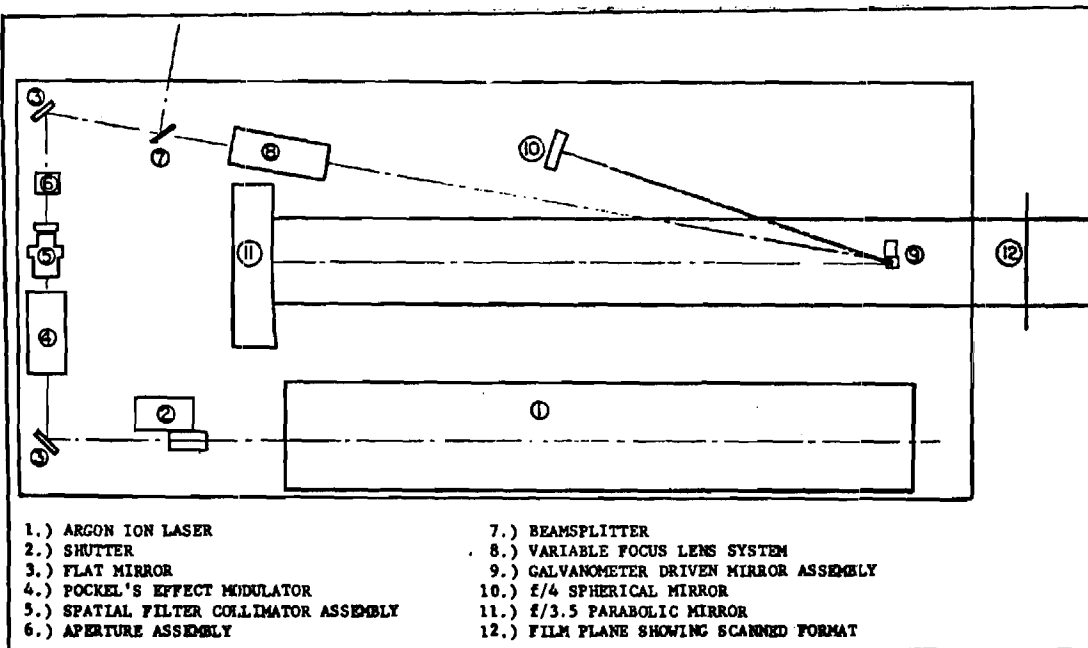


Fig. 3. Laser scanner optical system.

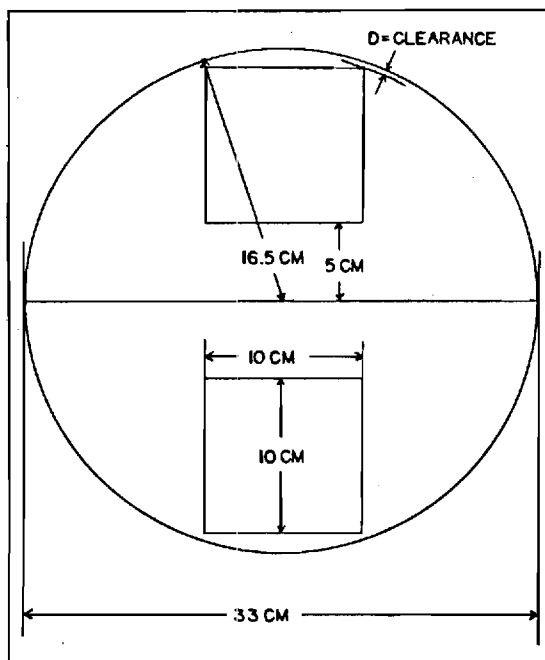
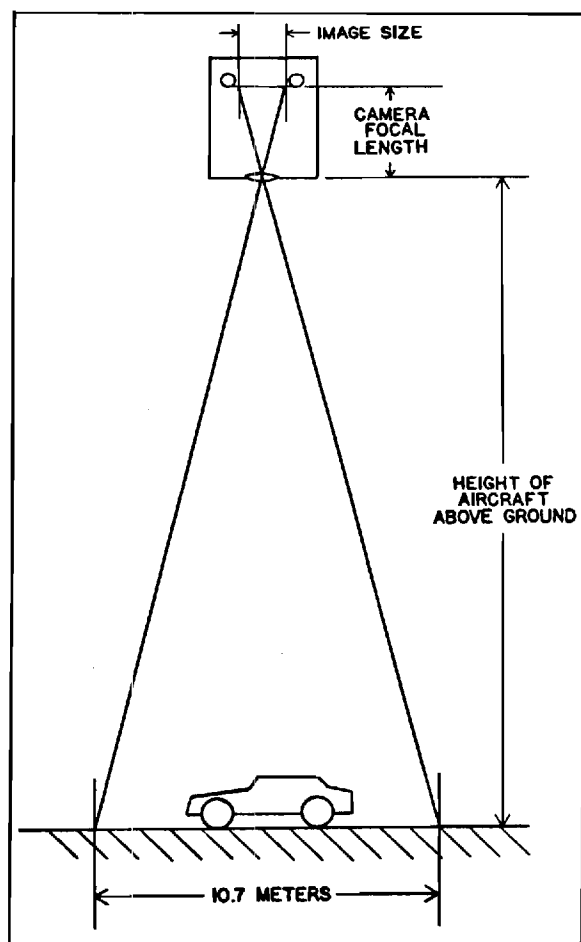


Fig. 4. Format projection on surface of parabolic mirror.

Fig. 5. Scaling of aerial photograph.



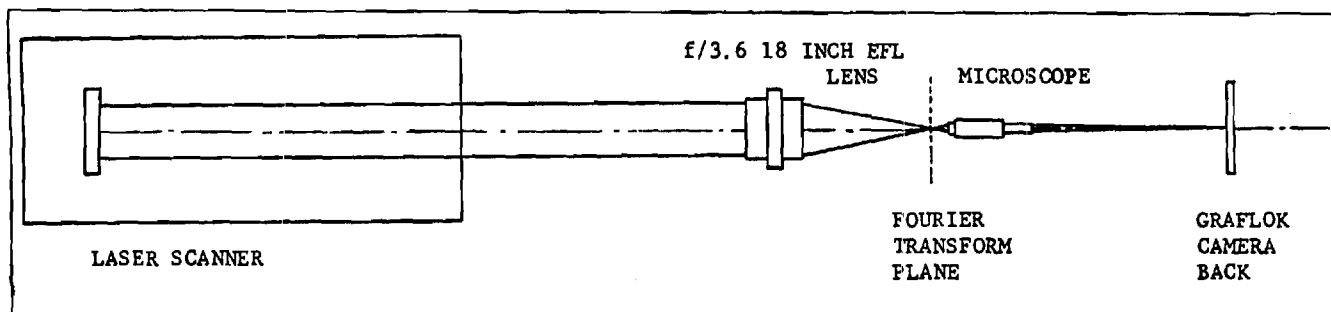


Fig. 6. (Above) Fourier transform spatial invariance test.

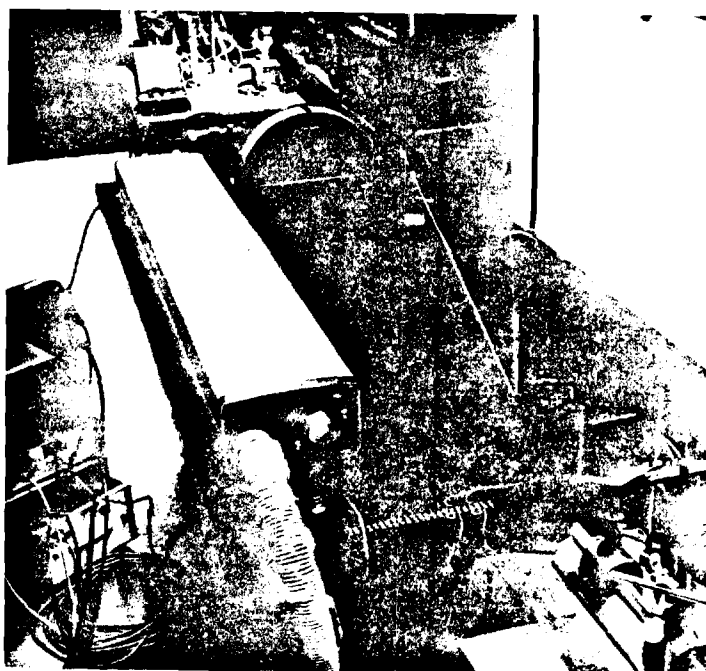
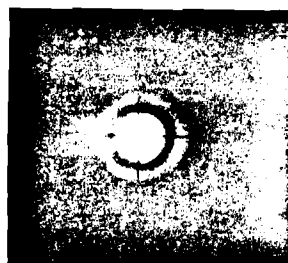
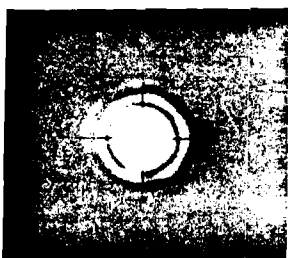


Fig. 8. Laser scanner during operational test. A single horizontal line is being traced by the scanner on the aerial photograph (lower right hand corner).



1.8 — DIAMETER CIRCULAR APERTURE
63.5 DIAMETERS



2.7 — DIAMETER CIRCULAR APERTURE
63.5 DIAMETERS

Fig. 7. Photomicrographs of Fourier transform patterns obtained using test apparatus of Fig. 6.

V. ACKNOWLEDGEMENTS

We would like to express our appreciation for the cooperation of Mr. H. Frayne Smith, Mr. Joseph Kerr, and Mr. Ellington Pitts of NASA/MSFC and Mr. John York of Sperry Rand Corporation.

REFERENCES

- [1] J. D. Beasley, "Electrooptic laser scanner for TV projection display," Applied Optics, vol. 10, no. 8, pp. 1934-1936, August 1971.
- [2] I. Gorog, J. D. Knox, and P. V. Goedertier, "Television rate laser scanner I. General considerations," RCA Review, vol. 33, no. 4, pp. 623-666, December 1972.
- [3] I. Gorog, J. D. Knox, P. V. Goedertier, and I. Shillovsky, "Television rate laser scanner II. Recent developments," RCA Review, vol. 33, no. 4, pp. 667-673, December 1972.
- [4] W. R. Callen, J. E. Weaver, R. G. Shackelford and J. R. Walsh, "Development of a coherent light scanner," Final Report on NASA Contract NAS8-28591, October 1973.
- [5] W. R. Callen, J. E. Weaver, R. G. Shackelford, and J. R. Walsh, "A coherent light scanner for optical processing of large format transparencies," Proceedings of the Electro-Optical System Design Conference - 1975, Chicago: Industrial and Scientific Conference Management, Inc., November 1975, pp. 487-493.
- [6] J. David Zook, "Light beam deflector performance: a comparative analysis," Applied Optics, vol. 13, no. 4, pp. 875-887, April 1974.
- [7] A. Yariv, Introduction to Optical Electronics, Second Edition. New York: Holt, Rinehart, and Winston, Inc., 1971, pp. 337-353.
- [8] All About Bragg Angle Errors in Acousto-Optic Modulators and Deflectors. Springfield, VA: Isomet Corporation Application Note.
- [9] Operations and Maintenance Manual--Model D-100 Acousto-Optic Driver. Springfield, VA: Isomet Corporation, December 1976.
- [10] Instruction Manual for Isomet Series LD-401 Acousto-Optic Deflectors. Springfield, VA: Isomet Corporation, September 1974.
- [11] P. J. Brosens, "Fast retrace optical scanning," Electro-Optical Systems Design, vol. 3, no. 4, pp. 21-24, April 1971.
- [12] Robert Compton, "Optical scanners; comparisons and applications," Electro-Optical Systems Design, vol. 8, no. 2, pp. 16-32, February 1976.

- [13] H. M. Tenney and J. C. Purcupile, "Laser/galvo scanner design," Electro-Optical Systems Design, vol. 7, no. 10, pp. 40-45, October 1975.
- [14] Operating and Maintenance Manual for the Model 3003 Modulation System. Danbury, Connecticut: Coherent Associates, Inc.